Laws of Effluent Dispersion in the Steady-State Atmospheric Surface Layer in Stable and Unstable Conditions

S. A. LEBEDEFF AND S. HAMEED[1]

Institute for Space Studies, NASA Goddard Space Flight Center, New York, N. Y. 10025

(Manuscript received 2 October 1975, in revised form 19 January 1975)

ABSTRACT

The two-dimensional diffusion equation has been solved by an integral method to obtain the distribution of ground-level concentration of an inert effluent emitted from a semi-infinite area source in a steady-state and horizontally homogeneous atmospheric surface layer. Mean wind velocity and eddy diffusivity profiles derived from empirically determined flux-profile relations of Businger *et al.* (1971) for stable and unstable surface layers were used. It is found that concentration as a function of downwind distance can be described by a simple formula over distances of practical interest in surface layer dispersion. Corresponding results for a cross-wind infinite line source are obtained by simple differentiation. The concentration distribution is completely determined by the friction velocity u_*, the Monin-Obukhov length L, the roughness length z_0, and the effluent source strength Q. The generalization of the integral method needed to obtain accurate solutions of the diffusion equation with the given wind velocity and diffusivity profiles is discussed in an appendix.

1. Introduction

For the study of dispersion of inert effluents from area and infinite line sources, which is of particular interest in air pollution problems, one may neglect diffusion in the horizontal direction and write the diffusion equation as

$$u(z)\frac{\partial X}{\partial x}=\frac{\partial}{\partial z}K(z)\frac{\partial X}{\partial z}, \tag{1}$$

where $X(x,z)$ is the concentration of the effluent, $u(z)$ the mean wind velocity, and $K(z)$ the coefficient of turbulent diffusion. The wind is assumed to be directed along the x axis. Recently we have analyzed this equation with the approximations

$$u(z)=u_0z^{\alpha}, \quad K(z)=K_0z^{\beta}. \tag{2}$$

The exact solution of (1) with profiles (2) for area sources has been obtained (Lebedeff and Hameed, 1975b). We have also solved this problem using an integral method (Lebedeff and Hameed, 1975a; Hameed and Lebedeff, 1975). Comparisons with the exact solution show that the integral method yields accurate solutions of the diffusion equation for area sources in all regimes of (α,β) of practical interest. The power law representation of $u(z)$ and $K(z)$ provides a useful approximation to the surface layer profiles under many conditions and has been extensively used in micrometeorology (Pasquill, 1974). In recent years, however, field measurements have been carried out which when combined with Monin–Obukhov's similarity theory give more realistic parameterizations of the surface layer. In this paper we will apply the integral method to solve the diffusion equation with such empirically obtained profiles of $u(z)$ and $K(z)$. We will find that the surface distribution of concentration downwind of an area or a crosswind line source can be described by simple laws.

The surface layer is the lowest part of the atmospheric boundary layer where the vertical fluxes of momentum, heat and moisture are approximately constant. For steady-state conditions, and with homogeneity in the horizontal direction, Monin–Obukhov similarity theory shows that $u(z)$ and $K(z)$ are determined by a function $\varphi(z/L)$:

$$\frac{kz}{u_*}\frac{\partial u(z)}{\partial z}=\varphi_m(z/L)=\frac{ku_*z}{K(z)}, \tag{3}$$

where u_* is the friction velocity, k the von Kármán constant, and L the Monin–Obukhov stability length. Most data from field measurements are found to be well represented if the function φ is written as [see, e.g., Businger *et al.* (1971); Paulson (1970); Webb (1970)]

$$\varphi=\begin{cases}1+\beta z/L, & L\geqslant 0\\ (1-\gamma z/L)^{-0.25}, & L\leqslant 0.\end{cases} \tag{4}$$

Some empirical estimates of the parameters β, γ, k are shown in Table 1.

[1] Senior Resident Research Associate of the National Academy of Sciences.

TABLE 1. Estimated values of parameters in the flux-profile relationships (3) and (4).

	β	γ	k
Businger *et al.* (1971)	4.7	15	0.37
Paulson (1970)	7	16	0.4
Webb (1970)	5.2	18	0.41

The depth of the surface layer is not uniquely defined but is usually of the order of several tens of meters. The lower boundary is taken at $z=z_0$, the local roughness length. Thus if z_0, u_* and L are known, the turbulent characteristics of the surface layer are completely specified through Eqs. (3) and (4). Solution of the diffusion equation with these profiles is therefore expected to give more realistic estimates of pollution dispersion in the surface layer than with the power law profiles of Eq. (2). The limited vertical range of applicability of these profiles restricts application to small horizontal distances, especially under unstable conditions. However, since the dynamics of the planetary boundary layer above the surface layer is more complicated and not as well determined, we will confine our attention to the study of dispersion in the surface layer in this paper. Also, since relations (3) and (4) have been verified only for steady-state and horizontally homogeneous conditions they are not applicable to typical urban atmospheres which are characterized by spatial variations in surface roughness and thermal effects. Our aim in this paper is, first, to show that the integral method can be extended to solve the diffusion equation with profiles of $u(z)$ and $K(z)$ more general than the power laws of Eq. (2) and, second, to solve the diffusion equation with empirically determined profiles of $u(z)$ and $K(z)$ so that the predicted concentration distributions could be compared with diffusion experiments.

We will consider a semi-infinite area source extending from $x=0$ to $x=\infty$. The emission of effluent is assumed to be uniform and constant, given by the condition

$$K(z)\frac{\partial X}{\partial z}=-Q\theta(x), \quad z=z_0, \tag{5}$$

where $\theta(x)$ is the step function:

$$\theta(x)=\begin{cases}0 & \text{for } x<0\\ 1 & \text{for } x\geq 0.\end{cases}$$

We note that $\partial X/\partial x$ is also a solution of the diffusion equation (1). Differentiation of (5) with respect to x gives

$$K(z)\frac{\partial}{\partial z}\frac{\partial X}{\partial x}=-Q\delta(x), \quad z=z_0, \tag{6}$$

where $\delta(x)$ is the Dirac delta function. Eq. (6) describes the emission of a constant effluent flux by an infinite line source located at $x=0$. Thus the solution of the line source problem is obtained from that of the area source by differentiation with respect to x. For this reason we will first obtain the solution of the diffusion equation for an area source.

Eq. (1) has been solved previously for an infinite line source by several authors who employed numerical methods. Yamamoto and Shimanuki (1961) used a "generalized mixing length theory" and obtained the function $\varphi(z/L)$ from

$$\varphi^4+(z/L)\varphi^3-1=0.$$

Yordanov (1973) has used K profiles in the surface layer similar to (3) and (4) but with a constant value of wind velocity. Ragland and Pierce (1975) solved the problem for a finite width line source, included diffusion in the y direction, and considered the wind direction parallel and at 45° to the source, in addition to being at right angles to it. Dispersion from a volume source, i.e., an area source with an assigned depth, has been numerically modeled by Egan and Mahoney (1972). As mentioned earlier, we will approach the problem using the integral method. One advantage of the method compared to the numerical techniques is the considerable reduction in labor. Also, uncertainties and errors encountered in the numerical solution of the partial differential equation (1) due to the singularity at the line source are avoided (see Yamamoto and Shimanuki, 1961). In the next section we formulate the problem and develop its solution by the integral method. Results are presented in Section 3 and conclusions in Section 4. Some aspects of the integral method of interest to the present problem are summarized in the Appendix.

2. Solution of the diffusion equation by the integral method

The similarity functions (4) define the mean profile distributions in the surface layer for arbitrary stability [Eq. (3)]. Thus

$$K(\zeta)=ku_*L\zeta/\varphi_m(\zeta), \quad \text{where} \quad \zeta=z/L, \tag{7}$$

and

$$u(\zeta)=\frac{u_*}{k}\int_{\zeta_0}^{\zeta}d\zeta\frac{\varphi_m(\zeta)}{\zeta}=\frac{u_*}{k}[f_m(\zeta)-f_m(\zeta_0)], \tag{8}$$

where

$$\zeta_0=z_0/L,$$

$$f_m(\zeta)=\begin{cases}\ln\zeta+\beta\zeta, & L>0\\ 2\ln^{-1}(1-\gamma\zeta)^{\frac{1}{2}}-\ln\left|\dfrac{1+(1-\gamma\zeta)^{\frac{1}{2}}}{1-(1-\gamma\zeta)^{\frac{1}{2}}}\right|, & L<0.\end{cases}$$

Defining

$$\xi=k^2\frac{x}{L}, \quad N=\frac{ku_*}{Q}X, \quad F_m(\zeta)=\frac{\zeta}{\varphi_m(\zeta)},$$

the diffusion equation (1) with mean wind velocity and diffusivity given by (7) and (8) may be written as

$$[f_m(\zeta)-f_m(\zeta_0)]\frac{\partial N}{\partial \xi}=\frac{\partial}{\partial \zeta}F_m(\zeta)\frac{\partial N}{\partial \zeta}, \tag{9}$$

and the flux boundary condition (5) becomes

$$F_m(\zeta)\frac{\partial N}{\partial \zeta}=-1, \quad \zeta=\zeta_0. \tag{10}$$

We also have the condition that concentration at the upwind edge of the area source is zero, i.e.,

$$N(0,\zeta)=0. \tag{11}$$

Once the velocity and diffusivity functions f_m and F_m are specified the problem posed in Eqs. (9)–(11) depends on only one external parameter ζ_0. The functions f_m and F_m, obtained using the parameters given by Businger *et al.* (1971), are displayed in Figs. 1a and b. The difference between the stable and unstable cases increases with increase in z/L; thus, the wind velocity is larger and the diffusivity smaller in the stable case in comparison with the unstable case. Thus we may expect that, for a given z/L, the effluents would have a shallower vertical spread in the stable case; this shallow layer would, however, be subjected to a stronger wind and would be carried to greater distances downwind.

In order to apply the integral method to the solution of (9)–(11), we first note that $F_m(\zeta)=\zeta/\varphi_m(\zeta)$ varies linearly with ζ near $\zeta=0$, for both $L>0$ and $L<0$.

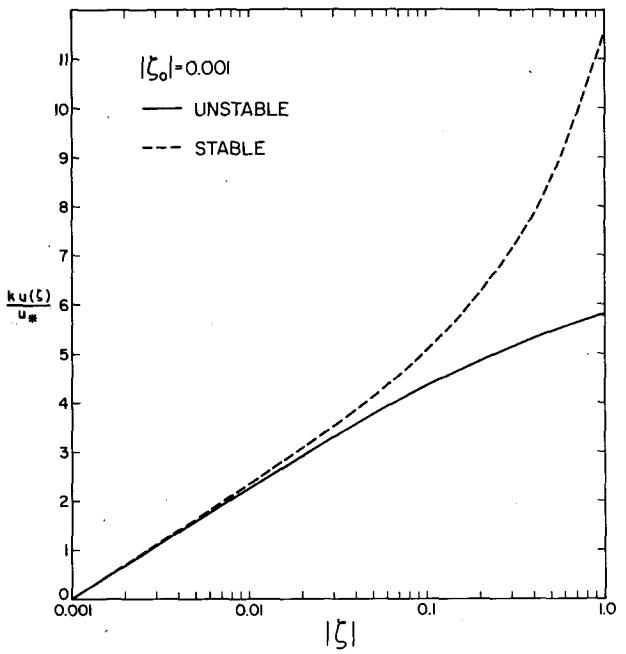

FIG. 1a. Vertical profile of the mean wind velocity.

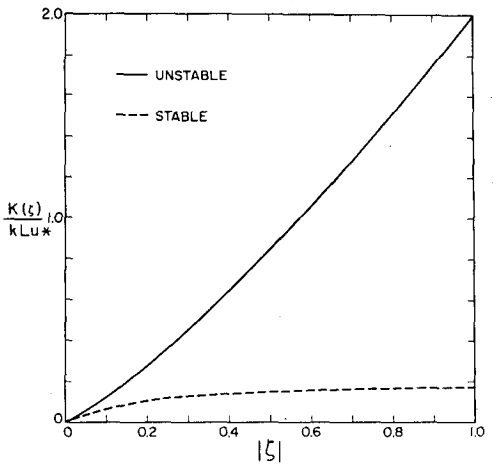

FIG. 1b. Vertical profile of the diffusion coefficient.

[See Eq. (4), the definition of $\varphi_m(\zeta)$.] It is therefore convenient to introduce the variable

$$\omega=\exp[f_m(\zeta)-f_m(\zeta_0)], \tag{12}$$

in terms of which (9)–(11) are written

$$U_m(\omega)\frac{\partial N}{\partial \xi}=\frac{\partial}{\partial \omega}\omega\frac{\partial N}{\partial \omega}, \tag{9a}$$

$$\omega\frac{\partial N}{\partial \omega}=-1, \quad \omega=1, \tag{10a}$$

$$N(0,\omega)=0, \tag{11a}$$

where

$$U_m(\omega)=\ln\omega\Big/\left(\frac{d\omega}{d\zeta}\right)=\frac{\zeta[f_m(\zeta)-f_m(\zeta_0)]}{\varphi_m(\zeta)\exp[f_m(\zeta)-f_m(\zeta_0)]}. \tag{13}$$

In Eq. (9a), the effective diffusivity is ω while the effective wind velocity profile appears as $U_m(\omega)$. From the discussion in the Appendix we know that when diffusivity is a linear function an accurate solution of the diffusion equation is obtained if we use the Ansatz:

$$N(\xi,\omega)=-\eta(\xi)\left(1-\frac{\omega}{\Delta}\right)^2\ln\left(\frac{\omega}{\Delta}\right), \quad \Delta\geqslant 1, \tag{14}$$

where the minus sign has been introduced for convenience. $\Delta(\xi)$ represents the depth of the contaminated layer in the ω space outside of which effluent density N and its vertical flux are taken to be zero; $\Delta\geqslant 1$ because the coordinate $\omega=1$ at the lower boundary z_0.

Application of the flux condition (10a) to (14) then gives

$$\eta(\xi)=\frac{\Delta^2}{(\Delta-1)(\Delta-1+2\ln\Delta)}. \tag{15}$$

Substituting this expression in (14) and taking $\omega=1$

then yields the required concentration at the surface $z=z_0$:

$$N_0(\xi)=\frac{(\Delta-1)\ln\Delta}{(\Delta-1+2\ln\Delta)}. \tag{16}$$

To solve for $\Delta(\xi)$ we integrate (9a) from $\omega=1$ to $\omega=\Delta$ to obtain

$$\frac{\partial}{\partial\xi}\int_1^{\Delta} U_m(\omega)N(\xi,\omega)d\omega=\omega\frac{\partial N}{\partial\omega}\Big|_{\omega=1}^{\omega=\Delta}=1$$

using (10a) and (A2). Integration over ξ now gives

$$-\eta(\Delta)\int_1^{\Delta} U_m(\omega)\left(1-\frac{\omega}{\Delta}\right)^2\ln\left(\frac{\omega}{\Delta}\right)d\omega=\xi, \tag{17}$$

where Δ is the effective depth of the contaminated layer in ω space. Let the corresponding depth in ζ space be δ. From Eq. (12) we then have

$$\Delta=\exp[f_m(\delta)-f_m(\zeta_0)]. \tag{18}$$

Using Eqs. (12) and (13), Eq. (17) now becomes

$$-\eta(\Delta)\int_{\zeta_0}^{\delta}[f_m(\zeta)-f_m(\zeta_0)]\left(1-\frac{\omega}{\Delta}\right)^2\ln\left(\frac{\omega}{\Delta}\right)d\zeta=\xi, \tag{17a}$$

where

$$\frac{\omega}{\Delta}=\exp[f_m(\zeta)-f_m(\delta)],$$

from (12) and (18). Since δ physically represents the depth of the polluted layer it is a monotonically increasing function of ξ. It is thus straightforward to calculate the left-hand side of (17a) for successively increasing values of δ and obtain the relationship between δ and ξ, and hence the surface concentration $N_0(\xi)$ by (16).

3. Results and discussion

By means of the method described in the previous section for an area source we have computed concentration as a function of downwind distance for a number of values of ζ_0, ranging between 0.1 and -0.1. We find that the differences between the predictions of the different parameterizations of the function $\varphi(z/L)$ given in Table 1 are small. For $L>0$, the use of Paulson's value of $\beta=7$ results in an overestimation of concentration by at most 10% in comparison with the Businger *et al.* and Webb models. For $L<0$, the differences between the three predictions are much smaller. For simplicity, in the following we will give results obtained with the parameter values of Businger *et al.* only. In Fig. 2a area source results are presented for different values of ζ_0 in the format of a log-log plot of surface concentration N_0 vs $\xi/\zeta_0=k^2x/z_0$. The following features are noteworthy in this figure:

1) Concentration at a downwind distance x is always larger in stable conditions as compared to unstable conditions.

2) Concentration at a given x increases with ζ_0 in the stable regime but decreases with increasing $|\zeta_0|$ in the unstable regime.

3) For very stable regimes, i.e., as ζ_0 becomes large, the curve in Fig. 2a tends to become a straight line. The departure from the straight line behavior increases as the stability decreases.

The approximate linearity of the curves in Fig. 2a suggests that they may be accurately represented by a

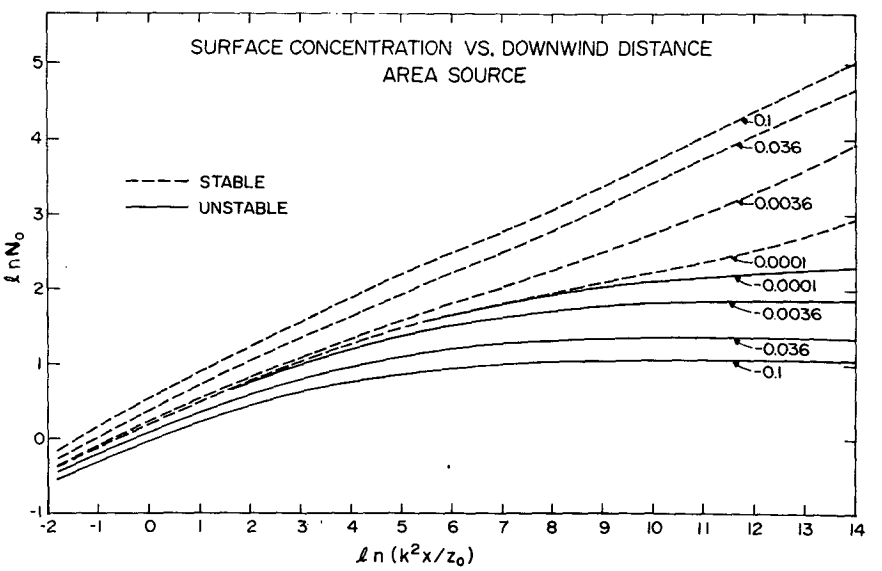

FIG. 2a. Predicted concentration at $z=z_0$ as a function of downwind distance for an area source.

rapidly converging series of the form

$$\ln N_0 = A + B\ln\xi + C(\ln\xi)^2 + D(\ln\xi)^3 + \ldots. \quad (19)$$

For each ζ_0 we have fitted the computed concentration with 2, 3, 4 and 5 terms in this series in the region $10^2 < k^2x/z_0 < 10^6$. (These limits roughly define the region of practical interest in observing dispersion in the surface layer.) We find that the contribution of the 4th and 5th terms in the series (19) is always small and the mean relative error is no more than 3% if they are neglected. We may therefore write

$$N_0(\xi) = e^A \xi^{B+C\ln\xi}. \quad (20)$$

The parameters A, B and C are functions of ζ_0 and are shown in Fig. 2b. We find that A, B and C are adequately approximated by the series

$$f = u + v\log_{10}|\zeta_0| + w(\log_{10}|\zeta_0|)^2. \quad (21)$$

The constants u, v and w are given in Table 2.

Reverting to dimensional coordinates, Eq. (20) gives for concentration at the surface $z = z_0$:

$$X(x,z_0) = \frac{Q}{ku_*} e^A \left[\frac{k^2x}{L}\right]^{B+C\ln(k^2x/L)}. \quad (20a)$$

This formula has been obtained for an area source extending from $x=0$ to $x=\infty$ with a uniform emission flux Q. A finite width source, which extends from $x=0$ to $x=x_1$ and is zero for $x>x_1$, can be represented as a superposition of two semi-infinite sources: the source with strength Q from $x=0$ to $x=\infty$ and a source with strength $(-Q)$ from $x=x_1$ to $x=\infty$, so that concentration for $x>x_1$ is given by

$$X(x,z_0) = \frac{Q}{ku_*} e^A \left\{\left[\frac{k^2x}{L}\right]^{B+C\ln(k^2x/L)} - \left[\frac{k^2(x-x_1)}{L}\right]^{B+C\ln[k^2(x-x_1)/L]}\right\}, \quad x>x_1. \quad (20b)$$

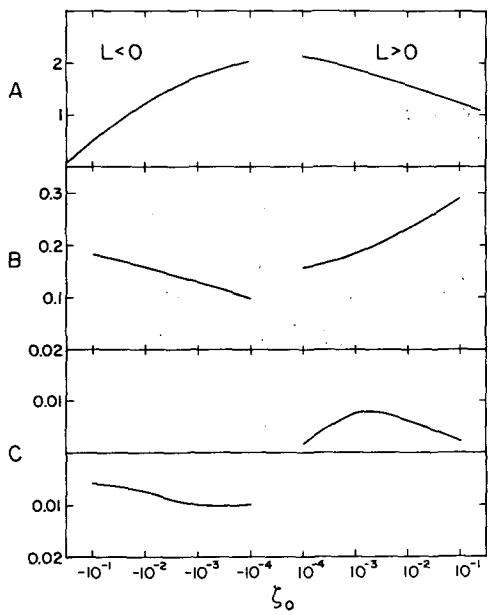

FIG. 2b. Dispersion coefficients A, B, C for an area source [Eq. (20)].

TABLE 2. Constants u, v, ω which determine the dispersion parameters A, B, C (area sources) and P, Q, R (line sources) through Eq. (21).

		u	v	ω
$L>0$	A	1.148	−0.2142	0.007255
	B	0.3633	0.08424	0.008037
	C	−0.008264	−0.01239	−0.002463
$L<0$	A	−0.08601	−0.8167	−0.07174
	B	0.06567	−0.04062	−0.008410
	C	−0.002014	0.004143	0.000552
$L>0$	P	−0.1761	−0.2602	−0.04611
	Q	−0.5667	0.1100	0.01067
	R	−0.008543	−0.007481	−0.0003049
$L<0$	P	−2.427	−1.160	−0.1627
	Q	−0.5760	0.2991	0.03915
	R	−0.09131	−0.02814	−0.002901

Area sources encountered in practice are in the form of grids with assigned values of source strength for different area intervals. Eq. (20) can be simply extended for such a source by representing it as a superposition of several semi-infinite area sources and using (20a) for each of them. An application of this procedure to an urban area source has been given by Lebedeff and Hameed (1975a). In general, for a variable source $Q(x)$ for $x_0 < x < x_1$, concentration at $z = z_0$ is given by the Riemann–Stieljes integral

$$X(x,z_0) = \frac{Q}{ku_*} e^A \int_0^{(x_1-x_0)} \left[\frac{k^2x}{L}\right]^{B+C\ln(k^2x/L)} dQ(x_1-x). \quad (20c)$$

As mentioned in Section 1 the concentration distribution for an infinite line source at right angles to the mean wind direction is obtained from the area source solution by differentiation with respect to x. Values of surface concentration N_0 for a line source obtained in this manner are shown in Fig. 3a as a plot of $\ln(LN_0/k^2)$ vs $\ln(k^2x/z_0)$. The following interesting features may be noted in this figure:

1) Very close to the source the concentration is primarily determined by the roughness length and not by the stability of the surface layer. Concentration at a given x is larger for smaller values of z_0.

2) As the effluent travels downwind the effect of atmospheric stability becomes more prominent. For a

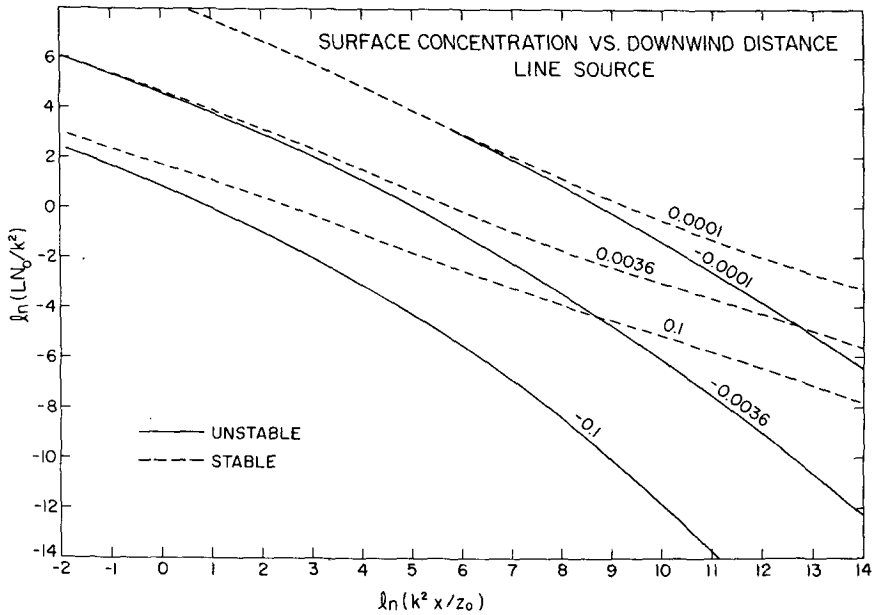

FIG. 3a. Predicted concentration at $z=z_0$ as a function of downwind distance from a line source. Note that for convenience the concentration has been multiplied by L/K^2.

given $|\zeta_0|$ the concentration becomes progressively larger for the stable case as compared to the unstable case.

3) The negative slope of the curves in Fig. 3a is largest for $\zeta_0=-0.1$ and smallest for $\zeta_0=+0.1$, i.e., for a given $|L|$, concentration as a function of a distance falls off most rapidly for large values of z_0 in unstable conditions and for small values of z_0 in stable conditions. These features of the dispersion curves may be explained by noting that the effect of an increase in the roughness length z_0 is to reduce values of surface concentration downwind. This is because the wind velocity becomes zero at $z=z_0$ [Eq. (8)] while the eddy diffusivity becomes zero at $z=0$ [Eq. (7)]. Thus if we compare two situations with different values of z_0, then near the surface the wind velocities in the two cases are the same but the eddy diffusivity is larger for the larger z_0. The larger diffusivity results in more rapid diffusion of the effiuent upward and therefore reduced concentrations at the surface. This explains the occurrence of smaller concentrations for larger values of $|\zeta_0|$ as noted in 1) above. The point noted in 2), that for a given $|\zeta_0|$ the concentration is larger in stable conditions in comparison with unstable conditions, is explained by the behavior of the diffusivity function as shown in Fig. 1b. The magnitude of the diffusivity increases much more sharply with height in the unstable case and this leads to smaller values of the surface concentration.

The property 3) of the line source distribution means that the downwind distance over which there is a significant accumulation of concentration is the shortest for large negative values of ζ_0 and longest for large positive ζ_0. Now an area source may be regarded as a large number of line sources placed adjacent to each other. This property of the line source therefore implies that in an area source, for large and negative ζ_0, each point would receive significant amounts of concentrations from only a small number of upwind line segments; the concentration would therefore be small in this case and would also increase slowly with x tending ultimately to a nearly constant value. In the opposite case of large and positive ζ_0 each line source segment contributes significantly over a long downwind distance; the concentration in the area source is therefore large and continues to build up rapidly as x increases. This behavior of the area source concentration distribution is clear in Fig. 2a.

We have fitted the line source concentration distributions with the series (19) in the region $10^2<k^2x/z_0<10^6$. Again, we find that three terms of the series are sufficient to represent the computed concentrations accurately so that we may write

$$N_0(\xi)=\frac{k^2}{L}e^P\xi^{Q+R\ln\xi}. \tag{22}$$

The parameters P, Q and R are shown in Fig. 3b. Values of the constants u, v and w required to represent P, Q, R by Eq. (21) are given in Table 2.

In Figs. 2b and 3b it is interesting to note that the dispersion parameters do not change smoothly as the stability changes from stable to unstable. This is perhaps a reflection, in the realm of dispersion phenomena, of the discontinuous structural changes that take place in the surface layer at the transition between the two stability regimes.

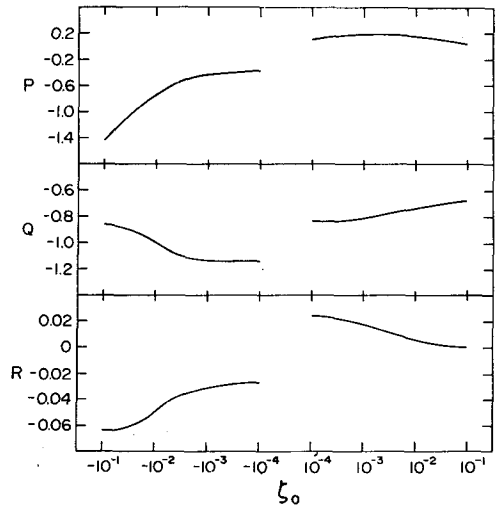

FIG. 3b. Dispersion coefficients P, Q, R for a line source [Eq. (22)].

We also note in Fig. 3a that as L becomes large the curves for $\pm\zeta_0$ tend to come together to form nearly a straight line, i.e., as one approaches neutral stability the contribution of the term $R\ln\xi$ in (22) becomes small and the concentration varies as ξ^Q. We find that $Q=-1.14$ for $\zeta_0=-0.0001$ and $Q=-0.83$ for $\zeta_0=+0.0001$. The average of these Q values is -0.99. It is well known that concentration from a line source varies approximately as x^{-1} under neutral conditions (Pasquill, 1974). Also, we note in Fig. 3b that R is negative for $L<0$, and positive for $L>0$. Thus in conditions different from neutral, the deviations from the simple power law behavior are such that the magnitude of the exponent $(Q+R\ln\xi)$ increases with x for $L<0$, and decreases with x for $L>0$. In stable conditions, however, as ζ_0 becomes large R approaches zero and a power law again becomes a good approximation. For comparison, we note that for an area source (Fig. 2b) the parameter B is always positive while C is negative for $L<0$ and positive for $L>0$. Thus as one departs from the neutral case the exponent $(B+C\ln\xi)$ increases with x for $L>0$ and decreases with x for $L<0$. Also C approaches zero as ζ_0 becomes large in the positive direction so that the concentration effectively increases as x^B in this regime.

The conclusions drawn in the previous paragraph about the power law behavior of the line source concentration distribution are in agreement with the results of the line source calculation of Yamamoto and Shimanuki (1961; see their Fig. 4). In Table 3 we compare line source concentrations at the surface predicted by our calculation with those given by Yamamoto and Shimanuki in their figures at several values of downwind distance. The difference between the two sets of values is small (generally well within a factor of 2) for the unstable case and for small ζ_0 in the stable case. The disagreement becomes significant for $\zeta_0=+0.01$. It is known, however, that the equation which was used by these authors to obtain φ gives erroneous results in stable conditions (Yamamoto and Shimanuki, 1966).

As discussed in Section 2 and in the Appendix it is assumed in the integral method that the effluent rises to a height $\delta(x)$, above which the concentration as well as the flux are taken to be zero. The function $\delta(x)$ therefore gives the shape of the effluent cloud in the integral

TABLE 3. Comparison of the prediction of line source concentration distribution by the calculation of Yamamoto and Shimanuki (1961) and the present calculation. The quantity tabulated is $LN_0\zeta_0/k^2$. Values given for Yamamoto and Shimanuki have been estimated from the figures in their paper.

		$L<0$		$L>0$	
$\lvert\zeta_0\rvert$	$\frac{x}{z_0}$	Yamamoto and Shimanuki (1961)	Integral method	Yamamoto and Shimanuki (1961)	Integral method
0.0001	125000	4.3×10^{-5}	4.3×10^{-5}	5.6×10^{-5}	3.7×10^{-5}
	25000	2.1×10^{-4}	2.6×10^{-4}	2.2×10^{-4}	1.1×10^{-4}
	5000	1.0×10^{-3}	1.4×10^{-3}	1.0×10^{-3}	1.4×10^{-3}
	1000	4.0×10^{-3}	6.4×10^{-3}	4.0×10^{-3}	7.0×10^{-3}
	625000			2.6×10^{-5}	5.0×10^{-5}
	125000	3.6×10^{-5}	2.3×10^{-5}	8.9×10^{-5}	1.5×10^{-4}
0.001	25000	1.9×10^{-4}	2.0×10^{-4}	2.3×10^{-4}	5.0×10^{-4}
	5000	1.0×10^{-3}	1.1×10^{-3}	1.0×10^{-3}	1.8×10^{-3}
	1000	4.0×10^{-3}	6.0×10^{-3}	4.2×10^{-3}	7.2×10^{-3}
	625000			5.1×10^{-5}	1.2×10^{-4}
	125000			1.4×10^{-4}	3.4×10^{-4}
0.01	25000	1.3×10^{-4}	8.8×10^{-5}	3.8×10^{-4}	1.0×10^{-3}
	5000	7.8×10^{-4}	6.7×10^{-4}	1.5×10^{-3}	3.2×10^{-3}
	1000	3.8×10^{-3}	3.9×10^{-3}	6.5×10^{-3}	1.0×10^{-2}

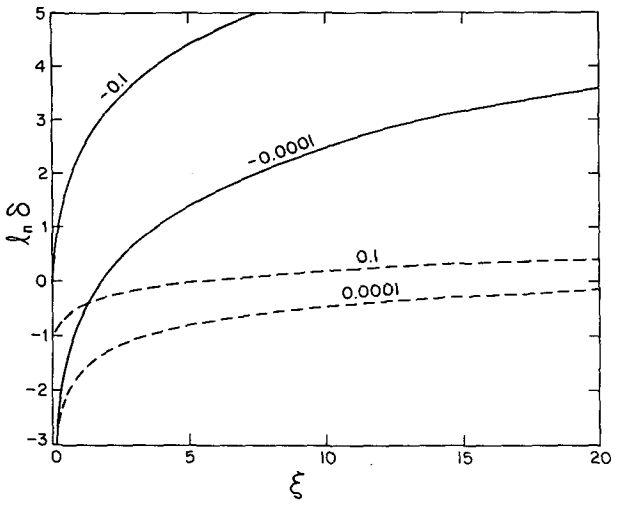

FIG. 4. The height of the polluted layer δ for different stability conditions.

method and this is shown in Fig. 4 for different values of ζ_0. As expected, we find that the cloud height is much larger in the unstable surface layer in comparison with the stable surface layer. Kazanskii and Monin (1957) have carried out experiments on dispersion of smoke emitted by a line source. They have photographed the shape of the smoke cloud under various stability conditions and their conclusions about the variation of cloud depth with ξ, and its dependence on stability, are qualitatively the same as presented in Fig. 4 (compare with their Figs. 12 and 6a). It may be noted here that the height $\delta(x)$ for an area source is the same as that for a line source because, again regarding the area source as a succession of line sources, the height of the effluent cloud from a particular line segment always remains lower than that of the preceding line segment; thus the height $\delta(x)$ for the area source is the same as that for the line which represents its upwind edge.

4. Conclusions

Using empirically derived vertical profiles for mean wind velocity and eddy diffusivity we have solved the two-dimensional diffusion equation to obtain the distribution of surface concentration of inert effluents from area and line sources in the horizontally uniform and stationary surface layer. The concentration distribution depends on the parameters u_*, L and z_0 and can be represented over distances of practical interest by the simple formulas (20) and (22).

The results are obviously limited by the reliability of the flux-profile parameterization of (3) and (4). These are expected to be good representations of steady-state conditions in open countryside where the terrain is nearly uniform; their validity for very different conditions, however, such as found in urban areas, is questionable. Also, although the surface layer is a useful approximation, it has interactions with the region above it, the neglect of which is also a limitation. Clearly, there is need for careful parameterizations of the atmospheric boundary layer under more general conditions. Study of urban boundary layers is of special interest for understanding air pollution dispersion. The study of dispersion in the surface layer, presented here, shows that availability of more realistic boundary layer profiles can have a significant impact on the feasibility of making air pollution forecasts under general conditions.

APPENDIX

Application of Integral Method to the Diffusion Equation

In the integral method one assumes a simple analytical form for the solution $X(x,z)$ in which the z dependence is explicitly specified. The solution is substituted in the diffusion equation and integrations over z carried out, resulting in an ordinary differential equation which yields $X_0(x)$, the surface concentration. This procedure is carried out subject to the boundary conditions and some additional constraints deduced from the nature of the problem. It is assumed that the diffusion of effluents in the z direction is limited to a depth $\delta(x)$ and that the flux outside this depth is zero:

$$X(x,z)=0, \quad z=\delta(x), \tag{A1}$$

$$\frac{\partial X(x,z)}{\partial z}=0, \quad z=\delta(x). \tag{A2}$$

The so called "smoothing condition" may also be imposed, i.e.,

$$\frac{\partial^2 X}{\partial z^2}=0, \quad z=\delta(x). \tag{A2'}$$

The accuracy of the solution obtained by the integral method obviously depends on the degree to which the assumed z profile of the solution simulates the true profile. To gain insight into the problem of choosing a suitable profile for the integral method it is instructive to consider the diffusion equation with the coefficients $u(z)$ and $K(z)$ given by the power laws of Eq. (2), because the exact solution of this problem is available for comparison. First, we note that if we integrate the diffusion equation (1) over z, the result depends on $K(z)$ only through its values at the boundaries, i.e., a solution obtained by the integral method does not incorporate the variation of K between the boundaries. It is therefore desirable to convert the equation to one with an effectively constant diffusivity by using the transformation

$$\omega=\int \frac{dz}{K(z)}. \tag{A3}$$

The flux boundary condition (5) now becomes

$$\frac{\partial X}{\partial \omega}=-Q, \quad \omega=0. \tag{A4}$$

When $K(z)=K_0 z^\beta$ [Eq. (2)], the transformation variable is

$$\omega=\frac{1}{K_0(1-\beta)}z^{1-\beta}, \tag{A5}$$

and the diffusion equation becomes

$$u_0 K_0[K_0(1-\beta)]^\mu \omega^\mu \frac{\partial X}{\partial x}=\frac{\partial^2 X}{\partial \omega^2}, \tag{A6}$$

where

$$\mu=(\alpha+\beta)/(1-\beta).$$

The usual integral method approach is to assume that the vertical profile may be approximated by a polynomial. A simple example of a polynomial which satisfies the compatibility relations (A1)–(A2′) is the cubic:

$$X_A=X_{A0}\left(1-\frac{\omega}{\delta}\right)^3, \tag{A7}$$

where $X_{A0}(x)$ is the concentration at $\omega=0$. Application of the integral method then gives (Lebedeff and

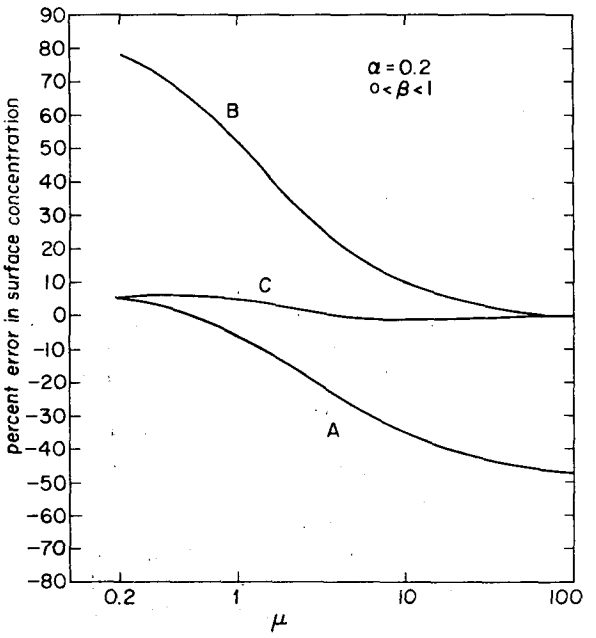

FIG. A1. Percent error in the predicted surface concentration as a function of $\mu=(\alpha+\beta)/(1-\beta)$ for three different assumed vertical profiles of concentration: A, the cubic profile [Eq. (A7)]; B, the profile of Eq. (A13); and C, the profile of Eq. (A15).

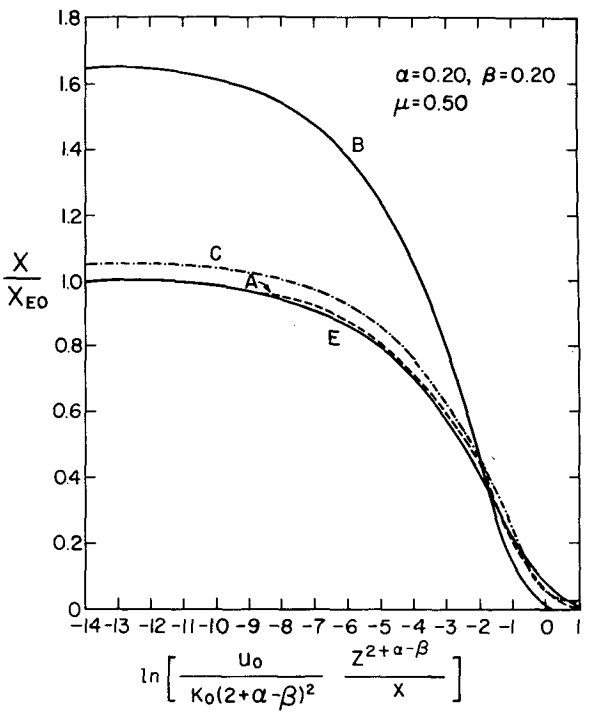

FIG. A2. Comparison of the three assumed profiles with the exact solution very close to the surface for a small value of μ.

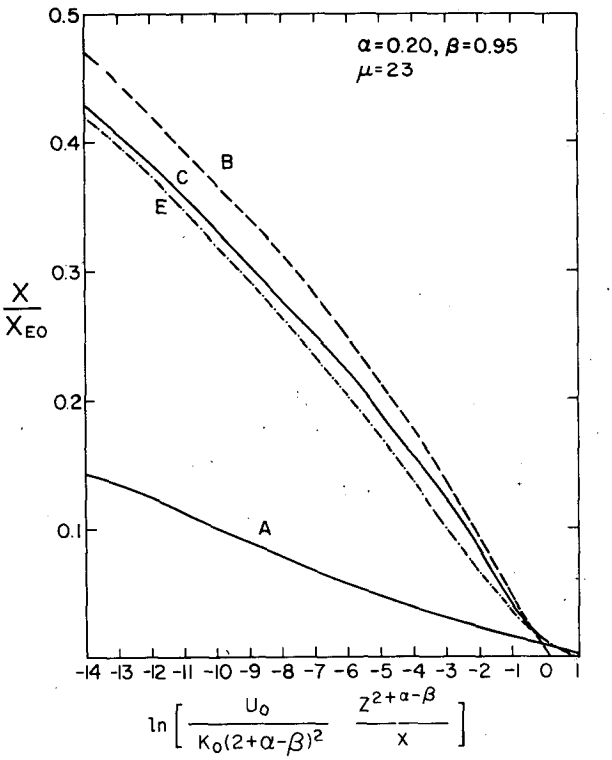

FIG. A3. As in Fig. A2 except for a large value of μ.

Hameed 1975a, 1976)

$$X_{A0}(x)=\frac{Q}{3}\left[\frac{3x}{u_0K_0^{1+\mu}(1-\beta)^{\mu}B(1+\mu,\,4)}\right]^{1/(2+\mu)}, \quad \text{(A8)}$$

where $B(a,b)$ is the beta function. The exact solution of this problem is (Lebedeff and Hameed, 1975b)

$$X_E(x,z)=X_{E0}(x)\frac{y^{1/(2+\mu)}}{(2+\mu)}\Gamma(-\nu,\,y), \quad \text{(A9)}$$

where

$$y=\frac{u_0}{K_0(2+\alpha-\beta)^2}\frac{z^{2+\alpha-\beta}}{x}$$

and $\Gamma(a,b)$ is the incomplete gamma function. For concentration at $z=0$, this yields

$$X_{E0}(x)=\frac{Q}{K_0}\frac{1}{(1-\beta)\Gamma\left(\frac{1+\mu}{2+\mu}\right)}\times\left[\frac{(2+\alpha-\beta)^2K_0x}{u_0}\right]^{1/(2+\mu)}. \quad \text{(A10)}$$

Note that the x dependence of the two solutions X_{A0} and X_{E0} is the same; the constant multiplying $x^{1/(2+\mu)}$ is different in the two expressions. The percent error in X_{A0} as a function of μ is shown as curve A in Fig. A1. The error is seen to be small for $\mu\ll1$ but increases progressively as μ increases to larger values. One may therefore suspect that the Ansatz (A7) of the cubic profile becomes inappropriate for $\mu\gg1$. This may be seen in Figs. A2 and A3 where the shape of the cubic profile near $\omega=0$ (curve A) is compared with that of the exact solution (curve E). For each profile X, the quantity X/X_{E0} has been plotted as a function of $\ln y$, so that the curves represent the z distribution of concentration for a given x. Note that in Fig. A2, with $\mu=0.5$, the profile of the exact solution decreases smoothly from 1 and the cubic profile follows it closely. In Fig. A3, on the other hand, with $\mu=23$, the profiles drop sharply near $y=0$ and the cubic profile differs considerably from the exact solution. Thus a simple polynomial in ω is not flexible enough to represent the solution in the neighborhood of $\omega=0$ for large μ.

It may be observed that for values of α and β of practical interest, the magnitude of $\mu=(\alpha+\beta)/(1-\beta)$ [and the error in solution (A8)] is much more sensitive to the value of β than to α. The difficulty of the cubic profile for large μ (i.e., $\beta\to1$) is therefore associated primarily with its inability to correctly account for the diffusion process. This is indicated also by the fact that as $\beta\to1$, $\omega=z^{1-\beta}/K_0(1-\beta)$ becomes ill-defined and the flux boundary condition is not satisfied.

From the definition (A3) we note that the proper variable for $\beta=1$ is $\omega=\ln z$. However if we choose a polynomial profile in terms of $\ln z$ we find that the flux condition cannot be satisfied. Lardner and Pohle (1961) applied the integral method to the equation

$$z\frac{\partial X}{\partial x}=\frac{\partial}{\partial z}z\frac{\partial X}{\partial z}, \quad \text{(A11)}$$

i.e., with $\alpha=\beta=1$, and showed that a profile which satisfies the boundary conditions and gives an accurate solution is

$$X(x,z)=X_0\left(1-\frac{z}{\delta}\right)^2\ln\left(\frac{z}{\delta}\right). \quad \text{(A12)}$$

Actually, this profile gives good solutions also for other values of α and β if $\beta\approx1$ and μ is large. For $\omega=z^{1-\beta}/K_0(1-\beta)$, the profile (A12) may be written

$$X_B=X_{B0}\left[1-\left(\frac{\omega}{\delta}\right)^{1/(1-\beta)}\right]^2\left(1-\frac{\omega}{\delta}\right), \quad \text{(A13)}$$

which gives, with the usual integral method procedure,

$$X_{B0}=Q\left[\frac{x}{u_0K_0^{1+\mu}(1-\beta)^{1+\mu}[B(1+\alpha,\,3)-B(2+\alpha-\beta,\,3)]}\right]^{1/(2+\mu)}. \quad \text{(A14)}$$

In Fig. A1 the percent error in this solution is shown as curve B. The error is less than 10% for $\mu>10$ but increases rapidly as μ becomes small. The suitability of profile (A13) for $\beta\approx1$ is apparent also from Figs. A2 and A3. It is seen to give a good approximation to the profile of the exact solution near $z=0$ for large μ in Fig. A3, but becomes inappropriate for small μ in Fig. A2. This profile correctly incorporates the singularity at $\beta=1$.

From this comparison it follows that a profile which reduces to (A7) for $\beta=0$ and to (A13) for $\beta=1$ would be suitable for use with the integral method for all values of β. One such profile is

$$X_C=X_{C0}\left[1-\frac{\omega}{\delta}\right]\left[1-(1-\beta)\frac{\omega}{\delta}-\beta\left(\frac{\omega}{\delta}\right)^{1/(1-\beta)}\right]. \quad \text{(A15)}$$

This gives

$$X_{C0}=\frac{Q}{(2-\beta)}\left[\frac{x}{u_0K_0^{1+\mu}(1-\beta)^{1+\mu}B}\right]^{1/(2+\mu)}, \quad \text{(A16)}$$

where

$$B=\frac{1}{(1+\alpha)}-\frac{\beta}{(2+\alpha)}-\frac{(2-\beta)}{(2+\alpha-\beta)}+\frac{\beta}{(3+\alpha-\beta)}-\frac{(1-\beta)}{(3+\alpha-2\beta)}.$$

In Fig. A1 it may be seen that the error in this solution, curve C, is very small for the whole range. This is because the profile (A15) gives a faithful representation of the exact solution near $z=0$, as shown in curves C in Figs. A2 and A3.

The diffusion equation (A6) represents a problem with an effectively constant diffusivity and an effective wind velocity which varies as ω^{μ}. The foregoing discussion of this problem covers the range $\mu=0$ to $\mu\to\infty$. {The case $\alpha=\beta=1$ [Eq. (A11)] corresponds to an effective velocity proportional to $e^{2\omega}$.} This encompasses the whole domain of problems in which $u(z)$ and $K(z)$ are represented by simple and continuous functions of z, and provides guidelines in choosing a suitable profile for the integral method.

To summarize, the choice of the profile depends on the behavior of the diffusivity function near the surface. In the surface layer problem [Eq. (9)] we note that $F_m(\zeta)\propto\zeta$ at $\zeta=0$. By means of the transformation (12) we preserve this behavior and cast the problem in the form possessing a linear diffusivity [Eq. (9a)] for which the profile (A12) gives accurate solutions.

REFERENCES

Businger, J. A., J. C. Wyngaard, Y. Izumi and E. F. Bradley, 1971: Flux-profile relationships in the atmospheric surface layer. *J. Atmos. Sci.*, **28**, 181–189.

Eagan, B. A., and J. R. Mahoney, 1972: Applications of a numerical air pollution transport model to dispersion in the atmospheric boundary layer. *J. Appl. Meteor.*, **11**, 1023–1039.

Hameed, S., and S. A. Lebedeff, 1975: Application of integral method to heat conduction in non-homogeneous media. *J. Heat Transfer, Trans. ASME*, **97**, 304–305.

Kazanskii, A. B., and A. S. Monin, 1957: The form of smoke jets. *Izv. Akad. Nauk SSSR, Ser. Geofiz.*, No. 8, 1020–1033. [See also Monin, A. S., 1959: Smoke propagation in the surface layer of the atmosphere. *Advances in Geophysics*, Vol. 6, 331–343.]

Lardner, T. J., and F. V. Pohle, 1961: Application of the heat balance integral to problems of cylindrical geometry. *Trans. ASME*, **28**, 310.

Lebedeff, S. A., and S. Hameed, 1975a: Study of atmospheric transport over area sources by an integral method. *Atmos. Environ.*, **9**, 333–338.

——, and ——, 1975b: Steady-state solution of the semiempirical diffusion equation for area sources. *J. Appl. Meteor.*, **14**, 546–549.

——, and ——, 1976: Study of atmospheric transport over area sources by an integral method: author's reply. *Atmos. Environ*, **10**, 170–171

Pasquill, F., 1974: *Atmospheric Diffusion*. Wiley, 429 pp.

Paulson, C. A., 1970: The mathematical representation of wind speed and temperature profiles in the unstable atmospheric surface layer. *J. Appl. Meteor.*, **9**, 857–861.

Ragland, K. W., and J. J. Pierce, 1975: Boundary layer model for air pollutant concentrations due to highway traffic. *J. Air Pollution Control Assoc.*, **25**, 48–51.

Webb, E. K., 1970: Profile relationships: The log-linear range, and extension to strong stability. *Quart J. Roy. Meteor. Soc.*, **96**, 67–90.

Yamamoto, G., and A. Shimanuki, 1961: Numerical solution of the equation of atmospheric turbulent diffusion. *Sci. Repts. Tohoku Univ.*, Ser. V, **12**, No. 1, 24–35.

——, and ——, 1966: Turbulent transfer in diabatic conditions. *J. Meteor. Soc. Japan*, Ser. II, **44**, 301–307.

Yordanov, D., 1973: Prediction of concentration patterns in the surface layer by synoptical information. *Proc. Third Intern. Clean Air Congress*, Dusseldorf, VDI-Verlag GmbH, B69–B71.